Inorg. Chem. **2005**, *44*, 3330–3336

Syntheses, Crystal Structures, and Magnetic Properties of Novel Manganese(II) Complexes with Flexible Tripodal Ligand 1,3,5-Tris(imidazol-1-ylmethyl)-2,4,6-trimethylbenzene

Wei Zhao,[†] You Song,[†] Taka-aki Okamura,[‡] Jian Fan,[†] Wei-Yin Sun,*[,†] and Norikazu Ueyama[‡]

Coordination Chemistry Institute, State Key Laboratory of Coordination Chemistry, Nanjing University, Nanjing 210093, China, and Department of Macromolecular Science, Graduate School of Science, Osaka University, Toyonaka, Osaka 560-0043, Japan

Received August 26, 2004

Two novel metal-organic frameworks (MOFs)—$[Mn(titmb)(N_3)_2]\cdot 1.5H_2O$ (**1**) and $[Mn_3(titmb)_2(C_2O_4)_3(H_2O)]\cdot 10H_2O$ (**2**)—were obtained by reactions of the flexible tripodal ligand 1,3,5-tris(imidazol-1-ylmethyl)-2,4,6-trimethylbenzene (titmb) with $Mn(OAc)_2\cdot 4H_2O$, together with NaN_3 and $K_2C_2O_4$, respectively. The structures of these MOFs were established by single-crystal X-ray diffraction analysis. The crystal data for **1** were as follows: monoclinic, *C*2/*c*, $a = 20.956(13)$ Å, $b = 9.884(6)$ Å, $c = 24.318(14)$ Å, $\beta = 95.87(5)°$, $Z = 8$. The crystal data for **2** were as follows: triclinic, $P\bar{1}$, $a = 12.400(9)$ Å, $b = 16.827(12)$ Å, $c = 17.196(11)$ Å, $\alpha = 66.35(5)$, $\beta = 95.87(5)°$, $\gamma = 71.03(6)$, $Z = 2$. Complex **1** is a novel noninterpenetrating three-dimensional (3D) framework, in which the azide ligand connects Mn^{II} atoms in an end-to-end (EE) mode to give $[Mn–N–N–N–]_n$ infinite one-dimensional (1D) chains, and complex **2** has a two-dimensional (2D) network structure in which the Mn^{II} ions are linked by the oxalate anions to form 1D $[Mn(C_2O_4)]_n$ chains. Each titmb in these two complexes connects three metal atoms and serves as a three-connecting ligand. The magnetic properties of **1** and **2** were investigated. The results showed that the antiferromagnetic interactions occurred between the Mn^{II} ions linked by the azide ligands in complex **1**, and those linked by the oxalate anions and the carboxylate in syn–anti coordination mode in complex **2**. The entirely different structures of complexes **1** and **2**, on one hand, indicate that the azide and the oxalate ligands affected the structures of MOFs greatly, and on the other hand, reveals the potential applications of MOFs with the azide and oxalate ligands, which are efficient magnetic couplers.

1. Introduction

The use of multidentate organic ligands and suitable metal salts to construct supramolecular architectures has been demonstrated to be a major strategy in recent years.[1] Metal-organic frameworks (MOFs) with specific topologies such as cagelike structures and honeycomb and interpenetrating networks have been obtained by reactions of suitable metal salts with rigid or flexible tripodal ligands that contain an aromatic core, for example 1,3,5-tricyanobenzene,[2] 2,4,6-tris(4-pyridyl)-1,3,5-triazine,[3] 1,3,5-benzenetribenzoate,[4] 1,3,5-tris(4-pyridylmethyl)benzene,[5] and 1,3,5-tris(benzimidazole-1-ylmethyl)-2,4,6-trimethylbenzene.[6] Supramolecular architectures have attracted much attention, not only because of their various structures, but also because of their potential applications.[7−11]

* To whom correspondence should be addressed. Tel.: +86-25-83593485. Fax: +86-25-83314502. E-mail: sunwy@nju.edu.cn.
[†] Nanjing University.
[‡] Osaka University.

(1) (a) Moulton, B.; Zaworotko, M. J. *Chem. Rev.* **2001**, *101*, 1629. (b) Kitagawa, S.; Kitaura, R.; Noro, S. *Angew. Chem., Int. Ed.* **2004**, *43*, 2334. (c) Leung, D. H.; Fiedler, D.; Bergman, R. G.; Raymond, K. N. *Angew. Chem., Int. Ed.* **2004**, *43*, 963. (d) Bu, X. H.; Tong, M. L.; Chang, H. C.; Kitagawa, S.; Batten, S. R. *Angew. Chem., Int. Ed.* **2004**, *43*, 192.
(2) Gardner, G. B.; Ventakaraman, D.; Moore, J. S.; Lee, S. *Nature* **1995**, *374*, 792.
(3) (a) Batten, S. R.; Hoskins, B. F.; Robson, R. *J. Am. Chem. Soc.* **1995**, *117*, 5385. (b) Abrahams, B. F.; Batten, S. R.; Hamit, H.; Hoskins, B. F.; Robson, R. *Angew. Chem., Int. Ed. Engl.* **1996**, *35*, 1690. (c) Abrahams, B. F.; Batten, S. R.; Grannas, M. J.; Hamit, H.; Hoskins, B. F.; Robson, R. *Angew. Chem., Int. Ed.* **1999**, *38*, 1475. (d) Batten, S. R.; Hoskins, B. F.; Moubaraki, B.; Murray, K. S.; Robson, R. *Chem. Commun.* **2000**, 1095.
(4) Chen, B. L.; Eddaoudi, M.; Hyde, S. T.; O'Keeffe, M.; Yaghi, O. M. *Science*, **2001**, *291*, 1021.
(5) Fujita, M.; Nagao, S.; Ogura, K. *J. Am. Chem. Soc.* **1995**, *117*, 1649.
(6) Su, C. Y.; Cai, Y. P.; Chen, C. L.; Lissner, F.; Kang, B. S.; Kaim, W. *Angew. Chem., Int. Ed.* **2002**, *41*, 3371.

10.1021/ic048816e CCC: $30.25 © 2005 American Chemical Society
Published on Web 04/05/2005

On the other hand, the azide (N_3^-) and oxalate ($C_2O_4^{2-}$) anions act not only as counterions but also as bridging ligands. Most recently, azide- and oxalate-containing coordination polymers have received considerable attention for the construction of new molecule-based magnets.[12−15] There are good reasons why the azide and the oxalate ligands are a subject of great interest. First, from the structural perspective, their diverse bridging modes can provide a series of novel MOFs. A second point of interest derives from the fact that they are efficient magnetic couplers. As a matter of fact, the azide ligand generally mediates antiferromagnetic interactions when it bridges metal atoms in an end-to-end (EE) mode, and ferromagnetic interactions in an end-on (EO) mode.[14a] As well, it has been demonstrated that the oxalate anions are useful to design and synthesize multi-functional and chiral magnets.[15] Because the magnetic behavior of exchange-coupled systems is greatly dependent on the frameworks, their dimensionality, and the topology, the ability to form transition-metal-azide (oxalate) coordination polymers is of utmost importance, but it still remains a great challenge.

There are reports on the magnetic properties of MOFs with rigid ligands.[16] For example, a novel mixed-valency $Cu^{II}Cu^{I}Cu^{II}$ triangular metallomacrocycle, using an imine-based rigid ligand, and the temperature dependence of the magnetic susceptibilities for this complex have been reported.[16a] However, in contrast to the rigid ligands with little or no conformational changes when they interact with metal salts, the flexible tripodal ligands have many more possible coordination modes, because of their flexibility, and they can adopt different conformations, according to the geometric requirements of different metal ions. We are interested in the reactions of flexible tripodal ligands with various metal salts to investigate the construction, structure, and property of MOFs.[17] Now, we initiate a study of the reactions of metal salts with the azide ligand or the oxalate ligand by incorporation of a tripodal bridging ligand. MOFs with novel structure and magnetic properties can be expected, because of the diversity of bridging modes of the azide, oxalate, and tripodal ligands, and the efficient mediating magnetic interactions of the azide and oxalate anions, as mentioned previously. As shown in Scheme 1, a flexible tridentate ligand (1,3,5-tris(imidazol-1-ylmethyl)-2,4,6-trimethylbenzene (titmb)) was adopted in this study, together with NaN_3 and $K_2C_2O_4$, to construct novel MOFs ($[Mn(titmb)(N_3)_2]\cdot 1.5H_2O$ (**1**) and $[Mn_3(titmb)_2(C_2O_4)_3(H_2O)]\cdot 10H_2O$ (**2**), respectively). Complex **1** is a novel noninterpenetrating three-dimensional (3D) framework, in which the azide ligand bridges Mn^{II} atoms in an EE mode, and complex **2** has a two-dimensional (2D) network structure in which the oxalate ligand links the Mn^{II} atoms to give one-dimensional (1D) chains. Here, we present the structures and magnetic properties of **1** and **2**.

Scheme 1. Schematic Drawing for Tripodal Ligand Titmb with cis, trans, trans-conformation

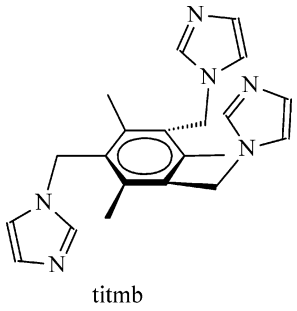

titmb

cis, trans, trans

2. Experimental Section

2.1. Materials and Measurements. All commercially available chemicals are reagent grade and used as received, without further purification. Solvents were purified according to the standard methods. C, H, and N analyses were made on a Perkin−Elmer model 240C elemental analyzer at the analysis center of Nanjing University. Infrared (IR) spectra were recorded on a Bruker model Vector22 FT-IR spectrophotometer, using KBr disks. Thermogravimetric and differential thermal analyses were performed on a simultaneous model SDT 2960 thermal analyzer. Magnetic measurements in the range of 1.8−300 K were performed on a MPMS−

(7) (a) Fiedler, D.; Leung, D. H.; Bergman, R. G.; Raymond, K. N. *J. Am. Chem. Soc.* **2004**, *126*, 3674. (b) Du, M.; Bu, X. H.; Guo, Y. M.; Ribas, J. *Chem.—Eur. J.* **2004**, *10*, 1345. (c) Muthu, S.; Yip, J. H. K.; Vittal, J. J. *J. Chem. Soc., Dalton Trans.* **2002**, 4561.
(8) Fan, J.; Gan, L.; Kawaguchi, H.; Sun, W.-Y.; Yu, K.-B.; Tang, W.-X. *Chem.—Eur. J.* **2003**, *9*, 3965.
(9) Fleming, J. S.; Mann, K. L. V.; Carraz, C. A.; Psillakis, E.; Jeffery, J. C.; McCleverty, J. A.; Ward, M. D. *Angew. Chem., Int. Ed.* **1998**, *37*, 1279.
(10) (a) Baxter, P. N. W.; Lehn, J.-M.; Baum, G.; Fenske, D. *Chem.—Eur. J.* **1999**, *5*, 102. (b) Baxter, P. N. W.; Lehn, J.-M.; Kneisel, B. O.; Baum, G.; Fenske, D. *Chem.—Eur. J.* **1999**, *5*, 113. (c) Tran, D. T.; Zavalij, P. Y.; Oliver, S. R. J. *J. Am. Chem. Soc.* **2002**, *124*, 3966.
(11) Yaghi, O. M.; Li, H.; Davis, C.; Richardson, D.; Groy, T. L. *Acc. Chem. Res.* **1998**, *31*, 474.
(12) Liu, C.-M.; Gao, S.; Zhang, D.-Q.; Huang, Y.-H.; Xiong, R.-G.; Liu, Z.-L.; Jiang, F.-C.; Zhu, D.-B. *Angew. Chem., Int. Ed.* **2004**, *43*, 990.
(13) (a) Kahn, O. *Molecular Magnetism*; VCH: Weinheim, Germany, 1993. (b) Gatteschi, D.; Kahn, O.; Miller, J. S.; Palacio, F. *Magnetic Molecular Materials*; NATO ASI Series, Vol. 198; Kluwer: Dordrecht, The Netherlands, 1991.
(14) (a) Ribas, J.; Escuer, A.; Monfort, M.; Vicente, R.; Cortés, R.; Lezama, L.; Rojo, T. *Coord. Chem. Rev.* **1999**, *193−195*, 1027. (b) Price, D. J.; Powell, A. K.; Wood, P. T. *J. Chem. Soc., Dalton Trans.* **2003**, 2478.
(15) (a) Pointillart, F.; Train, C.; Gruselle, M.; Villain, F.; Schmalle, H. W.; Talbot, D.; Gredin, P.; Decurtins, S.; Verdaguer, M. *Chem. Mater.* **2004**, *16*, 832. (b) Gruselle, M.; Andres, R.; Brissard, B. M. M.; Train, C.; Verdaguer, M. *Chirality* **2001**, *13*, 712. (c) Armentano, D.; Munno, G. D.; Lloret, F.; Palii, A. V.; Julve, M. *Inorg. Chem.* **2002**, *41*, 2007. (d) Coronado, E.; Clemente-León, M.; Galán-Mascarós, J. R.; Giménez-Saiz, C.; Gómez-García, C. J.; Martínez-Ferrero, E. *J. Chem. Soc., Dalton Trans.* **2000**, 3955. (e) Coronado, E.; Galán-Mascarós, J. R.; Gómez-García, C. J.; Laukhin, V. *Nature* **2000**, *408*, 447.
(16) (a) Guo, D.; Qian, C.-Q.; Duan, C.-Y.; Pang, K.-L.; Meng, Q.-J. *Inorg. Chem.* **2003**, *42*, 2024. (b) Barea, E.; Navarro, J. A. R.; Salas, J. M.; Masciocchi, N.; Galli, S.; Sironi, A. *Inorg. Chem.* **2004**, *43*, 473. (c) Lescouëzec, R.; Marinescu, G.; Vaissermann J.; Lloret, F.; Faus, J.; Andruh, M.; Julve, M. *Inorg. Chim. Acta* **2003**, *350*, 131. (d) Mendoza-Díaz, G.; Driessen, W. L.; Reedijk, J.; Gorter, S.; Gasque, L.; Thompson, K. R. *Inorg. Chim. Acta* **2002**, *339*, 51.
(17) (a) Fan, J.; Zhu, H.-F.; Okamura, T.; Sun, W.-Y.; Tang, W.-X.; Ueyama, N. *Chem.—Eur. J.* **2003**, *9*, 4724. (b) Fan, J.; Sui, B.; Okamura, T.; Sun, W.-Y.; Tang, W. X.; Ueyama, N. *J. Chem. Soc., Dalton Trans.* **2002**, 3868. (c) Wan, S.-Y.; Li, Y.-Z.; Okamura, T.; Fan, J.; Sun, W.-Y.; Ueyama, N. *Eur. J. Inorg. Chem.* **2003**, 3783. (d) Fan, J.; Zhu, H.-F.; Okamura, T.; Sun, W.-Y.; Tang, W. X.; Ueyama, N. *Inorg. Chem.* **2003**, *42*, 158. (e) Wan, S.-Y.; Fan, J.; Okamura, T.; Zhu, H.-F.; Ouyang, X.-M.; Sun, W.-Y.; Ueyama, N. *Chem. Commun.* **2002**, 2520.

Table 1. Crystal Data and Refinement Results for Complexes **1** and **2**

parameter	Value	
	1	**2**
chemical formula	$C_{21}H_{27}N_{12}MnO_{1.5}$	$C_{48}H_{70}N_{12}Mn_3O_{23}$
fw	526.49	1347.98
space group	*C*2/*c*	$P\bar{1}$
unit cell parameters		
a	20.956(13) Å	12.400(9) Å
b	9.884(6) Å	16.827(12) Å
c	24.318(14) Å	17.196(11) Å
α	90.00°	66.35(5)°
β	95.87(5)°	76.66(5)°
γ	90.00°	71.03(6)°
V	5011(5) Å^3	3087(4) Å^3
Z	8	2
λ	0.7107 Å	0.7107 Å
D_{calcd}	1.396 g/cm^3	1.450 g/cm^3
μ (Mo Kα) (mm^{-1})	0.569	0.689
temp, *T*	200 K	200 K
R^a	0.0442	0.0655
$R_w{}^b$	0.1005	0.0765

[a] $R = \Sigma||F_0| - |F_c||/\Sigma|F_0|$. [b] $R_w = |\Sigma w(|F_0|^2 - |F_c|^2)|/\Sigma|w(F_o)^2|^{1/2}$, where $w = 1/[\sigma^2(F_0^2) + (aP)^2 + bP]$. $P = (F_0^2 + 2F_c^2)/3$.

SQUID magnetometer under a field of 2 kG on powder samples in the temperature settle mode. The diamagnetic contributions of the samples were corrected using Pascal's constants.

Caution: Azide salts of metal complexes with organic ligands are potentially explosive and should be handled with care.

2.2. Preparation of the Complexes. 2.2.1. [Mn(titmb)(N_3)$_2$]·1.5H_2O (1). An aqueous solution (10 mL) of $Mn(OAc)_2{\cdot}4H_2O$ (12.3 mg, 0.05 mmol) and NaN_3 (6.5 mg, 0.1 mmol) was refluxed and stirred for ~8 h. The aqueous solution was filtrated and cooled to room temperature, and a solution of titmb (18.0 mg, 0.05 mmol) in acetonitrile (10 mL) was carefully layered over the aqueous solution at room temperature. About two weeks later, pale-yellow block crystals suitable for X-ray analysis were obtained in 50% yield. Anal. Calcd for $C_{21}H_{27}MnN_{12}O_{1.5}$: C, 47.91; H, 5.17; N, 31.93. Found: C, 47.82; H, 5.04; N, 31.86. IR (KBr, cm^{-1}): 3424 m, 3105 m, 2078 s, 1620 m, 1510 m, 1229 m, 1110 m, 1088 m, 1020 m, 931 m, 836 m, 765 m, 744 m, 659 m, 616 m.

2.2.2. [Mn_3(titmb)$_2$(C_2O_4)$_3$(H_2O)]·10H_2O (2). The title complex was also prepared by slow diffusion between two layers of the aqueous solution (10 mL) of the manganese(II) salt of the oxalate, obtained by the same procedures as those described previously from $Mn(OAc)_2{\cdot}4H_2O$ (12.3 mg, 0.05 mmol) and $K_2C_2O_4$ (18.4 mg, 0.1 mmol), and titmb (18.0 mg, 0.05 mmol) in methanol (10 mL) at room temperature. Single crystals suitable for X-ray analysis were obtained in 40% yield three weeks later. Anal. Calcd for $C_{48}H_{70}Mn_3N_{12}O_{23}$: C, 42.77; H, 5.23; N, 12.47. Found: C, 42.83; H, 5.18; N, 12.30. IR (KBr, cm^{-1}): 3424 m, 3127 m, 1617 s, 1512 m, 1452 m, 1310 m, 1225 m, 1109 m, 1089 m, 1025 m, 937 m, 828 m, 790 m, 766 m, 659 m, 618 m. The TGA data of **2** showed an initial weight loss of 15.0% (calcd. 14.7%) from 30 °C to 174 °C, representing the loss of all water molecules; no further weight loss was observed over the temperature range of 174−306 °C.

2.3. Crystallographic Analyses. The collections of crystallographic data for **1** and **2** were performed on a Rigaku RAXIS−RAPID Imaging Plate diffractometer at 200 K, using graphite-monochromated Mo Kα radiation ($\lambda = 0.7107$ Å). The structures were solved by direct methods with SIR92[18] and expanded using the Fourier technique.[19] All non-hydrogen atoms were refined anisotropically by the full-matrix least-squares method. The H atoms (except for those of water molecules) were generated geometrically. All calculations were performed on an SGI workstation using the teXsan crystallographic software package of Molecular Structure Corporation.[20] Details of the crystal parameters, data collection, and refinement are summarized in Table 1, and selected bond lengths and angles with their estimated standard deviations are listed in Table 2. Further details are provided in the Supporting Information.

Table 2. Selected Bond Distances and Angles for Complexes **1** and **2**[a]

Bond Distances (Å), **1**			
Mn1−N6	2.227(2)	Mn2−N4	2.228(2)
Mn1−N1	2.273(2)	Mn2−N32	2.288(2)
Mn1−N11	2.283(2)	Mn2−N52	2.303(2)

Bond Angles (deg), **1**			
N6#1−Mn1−N6	180.0	N6−Mn1−N1#1	90.39(9)
N6−Mn1−N1	89.61(9)	N1#1−Mn1−N1	180.0
N6#1−Mn1−N11	89.59(8)	N6−Mn1−N11	90.41(8)
N1#1−Mn1−N11	89.94(9)	N1−Mn1−N11	90.06(9)
N11−Mn1−N11#1	180.0	N4#2−Mn2−N4	180.0
N32#2−Mn2−N32	180.0	N4−Mn2−N32#2	86.21(8)
N4−Mn2−N52	94.24(9)	N4−Mn2−N32	93.79(8)
N32−Mn2−N52	86.44(8)	N32−Mn2−N52#2	93.56(8)
N4−Mn2−N52#2	85.76(9)	N52−Mn2−N52#2	180.0

Bond Distances (Å), **2**			
Mn1−O1	2.178(4)	Mn1−O3	2.220(4)
Mn1−N12	2.276(5)	Mn2−N52	2.261(5)
Mn2−O21	2.184(4)	Mn2−N32	2.187(5)
Mn2−O7	2.191(4)	Mn2−O2	2.197(4)
Mn2−O5	2.198(4)	Mn3−N112#3	2.247(6)
Mn3−O6	2.185(4)	Mn3−O8	2.185(4)
Mn3−N132#4	2.190(5)	Mn3−O9	2.201(4)
Mn3−O11	2.213(4)	Mn4−N152	2.241(5)
Mn4−O12	2.192(4)	Mn4−O10	2.214(4)

Bond Angles (deg), **2**			
O1(5)−Mn1−O1	180.0	O3−Mn1−O3#5	180.0
O1−Mn1−O3	75.79(15)	O1−Mn1−N12#5	90.56(17)
O1−Mn1−O3	104.21(15)	O3−Mn1−N12	92.30(16)
O3#5−Mn1−N12	87.70(17)	O1−Mn1−N12	89.44(17)
N12#5−Mn1−N12	180.0	O21−Mn2−N32	94.19(18)
O21−Mn2−O7	170.38(13)	N32−Mn2−O7	89.66(18)
O21−Mn2−O2	89.79(15)	N32−Mn2−O2	91.07(17)
O7−Mn2−O2	98.96(15)	O21−Mn2−O5	94.24(14)
N32−Mn2−O5	94.76(16)	O7−Mn2−O5	76.63(14)
O2−Mn2−O5	172.64(15)	O21−Mn2−N52	92.66(18)
N32−Mn2−N52	171.63(18)	O7−Mn2−N52	84.33(17)
O2−Mn2−N52	84.14(17)	O5−Mn2−N52	89.51(17)
O6−Mn3−O8	77.08(14)	O6−Mn3−N132#4	93.15(19)
O8−Mn3−N132#4	90.80(17)	O6−Mn3−O9	105.78(15)
O8−Mn3−O9	171.60(16)	N132#4−Mn3−O9	96.87(17)
O6−Mn3−O11	176.45(14)	O8−Mn3−O11	101.44(15)
N132#4−Mn3−O11	90.09(18)	O9−Mn3−O11	75.23(15)
O6−Mn3−N112#3	86.93(18)	O8−Mn3−N112#3	83.37(17)
N132#4−Mn3−N112#3	174.00(17)	O9−Mn3−N112#3	88.87(17)
O11−Mn3−N112#3	89.70(18)	O12−Mn4−O12#4	180.0
O12−Mn4−O10	75.62(14)	O12−Mn4−N152	90.50(17)
O12−Mn4−O10#4	104.38(14)	O10−Mn4−N152	88.53(17)
O10−Mn4−O10#4	180.0	N152#4−Mn4−N152	180.0
O12#4−Mn4−N152	89.50(17)	O10#4−Mn4−N152	91.47(17)

[a] Symmetry transformation used to generate equivalent atoms: #1, $1-x, 1+y, {}^1/_2-z$; #2, $1+x, -y, -{}^1/_2+z$; #3, $-x, 1-y, -z$; #4, $1-x, 1-y, -z$; #5, $-x, -y, 2-z$.

(18) Altomare, A.; Burla, M. C.; Camalli, M.; Cascarano, M.; Giacovazzo, C.; Guagliardi, A.; Polidori, G. SIR92. *J. Appl. Crystallogr.* **1994**, *27*, 435.

(19) Beurskens, P. T.; Admiraal, G.; Beurskens, G.; Bosman, W. P.; de Gelder, R.; Israel, R.; Smits, J. M. M. DIRDIF94: The DIRDIF-94 Program System, Technical Report of the Crystallography Laboratory, University of Nijmegen, The Netherlands, 1994.

(20) teXsan: Crystal Structure Analysis Package, Molecular Structure Corporation, The Woodlands, TX, 1999.

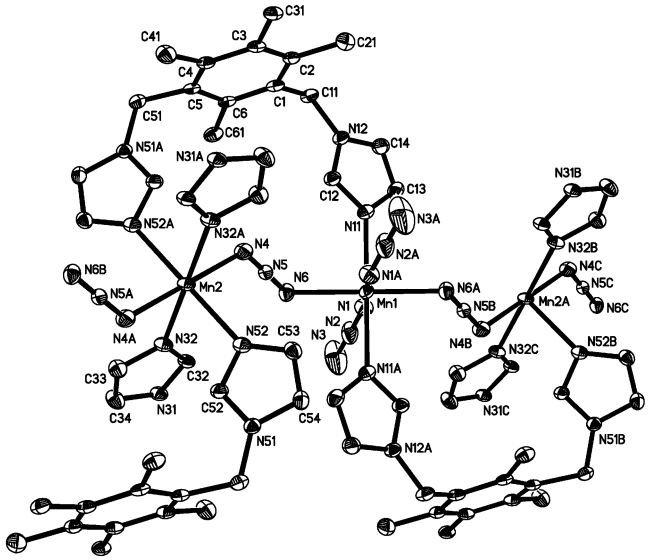

Figure 1. Coordination environment around the Mn^{II} atoms in compound **1** (the lattice water molecules and H atoms have been omitted for the sake of clarity). The thermal ellipsoids are drawn at 30% probability.

3. Results and Discussion

3.1. Description of Crystal Structures. 3.1.1. $[Mn(titmb)(N_3)_2]\cdot 1.5H_2O$ (1). Previous studies show that flexible tripodal ligands with an aromatic core are versatile bridging ligands and can form various MOFs with transition and main-group metal salts.[17] Complex **1** was readily prepared via a layering method, using titmb, $Mn(OAc)_2\cdot 4H_2O$ (OAc = acetate), and NaN_3. Pale-yellow block crystals of **1** conform to the space group *C2/c* with eight asymmetric units in one unit cell (see Table 1). The coordination environment around the Mn(II) centers is presented in Figure 1 with an atom numbering scheme, where the Mn^{II} atoms sit on the inversion center. There are two independent Mn^{II} atoms in an asymmetric unit of **1**. It is noteworthy that the two Mn^{II} atoms have different coordination environments. The Mn1 atom is coordinated by two N (N11 and N11A) atoms, from two imidazolyl groups of two different titmb ligands with the N11−Mn−N11B angle of 180° in a trans arrangement. Four additional positions are occupied by four N atoms of four different azide anions with $N_{azide}-Mn-N_{azide}$ bond angles ranging from 89.61(9)° to 180.0° and $Mn-N_{azide}$ bond distances of 2.227(2) and 2.273(2) Å, respectively, as listed in Table 2. The Mn2 atom is coordinated by four N atoms of imidazolyl groups from four individual titmb ligands, and by two N atoms of two different azide anions with Mn−N bond distances ranging from 2.228(2) Å to 2.303(2) Å and N−Mn−N bond angles varying from 85.75(9)° to 180.0°, as tabulated in Table 2. The local coordination environment around Mn(II) can be regarded as a slightly distorted octahedron, accordingly. In addition, each titmb ligand with cis, trans, trans-conformation (Scheme 1) connects three Mn^{II} atoms, serving as a three-connecting ligand. The azide anions containing atoms N4, N5, and N6 bridged Mn1 and Mn2 in an EE fashion with metal−metal separations (Mn1···Mn2) of 5.79 Å, whereas the azide anion containing atoms N1, N2, and N3 functions as a terminal ligand, rather than a bridging one.

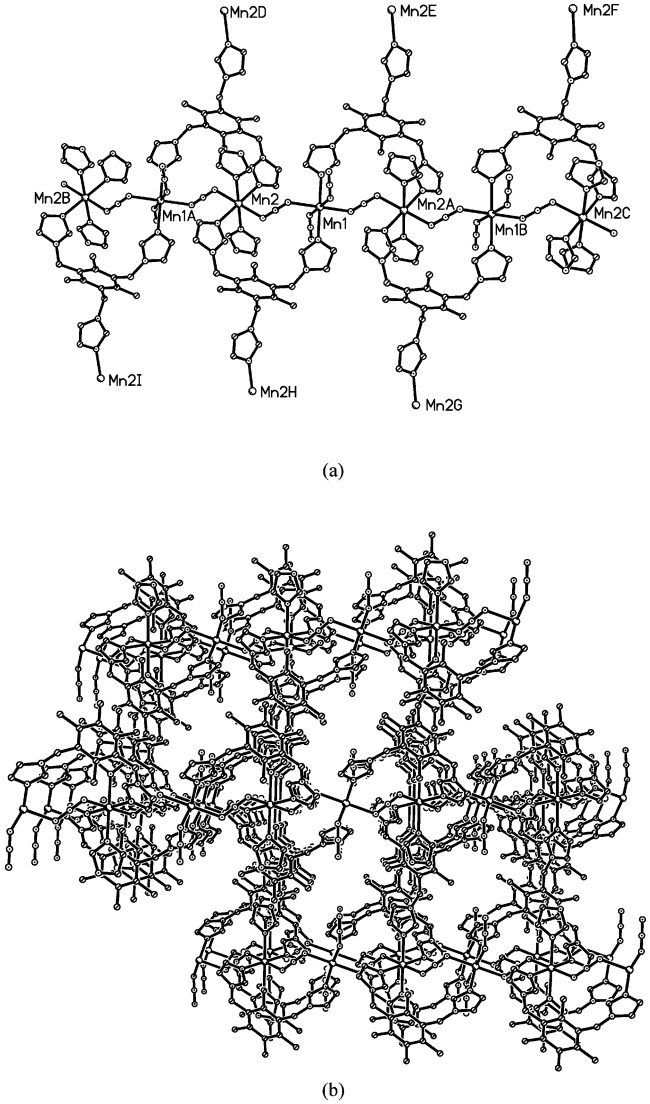

Figure 2. (a) Infinite one-dimensional (1D) chain structure of complex **1** linked by a N_3^- anion and a titmb ligand. (b) Three-dimensional (3D) structure of complex **1** (the lattice water molecules and H atoms have been omitted for clarity).

Neglecting the interactions of Mn(II) with the imidazolyl groups containing N32 and N32A, Mn1 and Mn2 atoms are linked by azide anions and titmb ligands to form extended 1D chains, as illustrated in Figure 2a. Adjacent 1D chains are arranged in different directions with an angle of 56.5° between the two adjacent 1D chains (see Figures S1 and S2 in the Supporting Information), and are further cross-linked by Mn2−N (imidazolyl groups containing N32 and N32A) bonds, leading to the formation of a 3D open framework, as represented in Figure 2b and Figure S3 in the Supporting Information. The crystal water molecules occupy the voids of the 3D framework and are held there by C−H···O and O−H···O hydrogen bonds (see Figure S4 in the Supporting Information). The H atoms connected to the O atom of water molecules were found in the difference Fourier map directly. The hydrogen bonding data for the complexes are summarized in Table 3.

3.1.2. $[Mn_3(titmb)_2(C_2O_4)_3(H_2O)]\cdot 10H_2O$ (2). Similar to the azide anion, the oxalate anion is also a versatile multidentate bridging ligand. When the reaction of the titmb

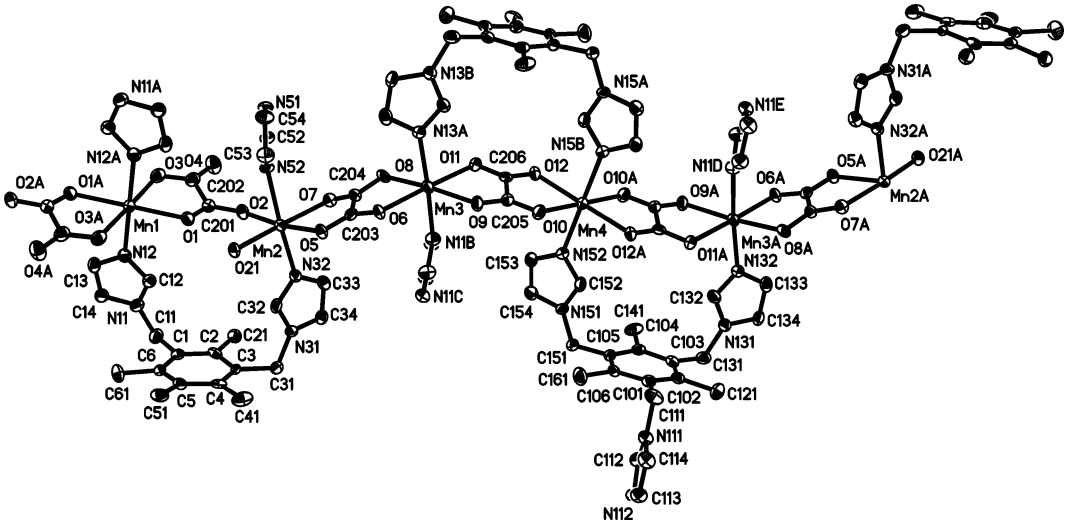

Figure 3. Coordination environment around the Mn^{II} atoms in complex **2** (the lattice water molecules and H atoms have been omitted for the sake of clarity). The thermal ellipsoids are drawn at 30% probability.

Table 3. Distance and Angles of Hydrogen Bonding for Complexes **1** and **2**[a]

D−H···A[b]	distance D···A[b] (Å)	D−H−A[b]	angle D−H−A[b] (deg)
	Compound **1**		
O(2)−H(26)···O(1)	3.443(5)	O(2)−H(26)−O(1)	151
O(2)−H(27)···N(3)#1	2.960(5)	O(2)−H(27)−N(3)#1	127
C(32)−H(11)···N(5)	3.280(4)	C(32)−H(11)−N(5)	127
C(32)−H(11)···N(6)	3.392(4)	C(32)−H(11)−N(6)	154
C(34)−H(13)···O(2)#2	3.246(4)	C(34)−H(13)−O(2)#2	145
C(51)−H(18)···N(6)#3	3.466(4)	C(51)−H(18)−N(6)#3	164
	Compound **2**		
C(41)−H(14)···N(51)#4	3.236(9)	C(41)−H(14)−N(51)#4	124
C(131)−H(34)···O(21)#5	3.556(8)	C(131)−H(34)−O(21)#5	172
C(151)−H(42)···O(40)#6	3.346(9)	C(151)−H(42)−O(40)#6	135
O(2)−O(36)#7	2.85		
O(4)−O(40)#8	2.79		
O(8)−O(35)#7	2.75		
O(21)−O(37)#9	2.65		
O(31)−O(39)#10	2.88		
O(3)−O(38)#8	2.85		
O(9)−O(39)#10	2.83		
O(31)−O(37)#10	2.79		
O(34)−O(35)#7	2.80		

[a] Symmetry transformation used to generate equivalent atoms: #1, $-1-x, -1+y, {}^{1}/_{2}-z$; #2, ${}^{3}/_{2}+x, {}^{1}/_{2}+y, z$; #3, $1+x, 1-y, -{}^{1}/_{2}+z$; #4, $-1+x, y, z$; #5, $x, 1+y, -1+z$; #6, $-x, 2-y, -z$; #7, $1-x, 1-y, 1-z$; #8, $x, -1+y, 1+z$; #9, $-x, 1-y, 1-z$; #10, $x, -1+y, z$. [b] D = donor and A = acceptor.

ligand with $Mn(OAc)_2{\cdot}4H_2O$ and $K_2C_2O_4$ was performed, **2** was successfully isolated. The crystallographic study provides direct evidence for the structure of **2**. As listed in Table 1, the complex crystallizes in the triclinic space group $P\bar{1}$, and Figure 3 shows the coordination environments of the Mn^{II} atom in **2** with an atom numbering scheme where the Mn1 and Mn4 reside on the inversion center. It is noteworthy that the asymmetric unit of **2** contains four distinct Mn(II) centers, in which Mn2 is coordinated by four O atoms from two different oxalate anions and one water molecule, whereas the Mn1, Mn3, and Mn4 atoms have the same coordination environments and each is coordinated by four O atoms from two different oxalate anions. The O−Mn−O bond angles vary from 75.23(15)° to 180.0° and Mn−O bond distances range from 2.178(4) Å to 2.220(4) Å, respectively (see Table 2). Interestingly, there are three oxalates in the asymmetric unit of **2** with two types of bridging modes. Namely, the oxalate with O1, O2, O3, and O4 coordinates to two Mn(II) as a bidentate, unidentate ligand, whereas the oxalate with O5, O6, O7 and O8, as well as that with O9, O10, O11, and O12, connects two Mn^{II} atoms as a bidentate, bidentate ligand. Such different bridging modes of the oxalate ligand have a difference in mediating magnetic coupling between the Mn^{II} ions (vide infra). In addition to the O atoms, each Mn^{II} atom is coordinated by two N atoms of the imidazole units from two different titmb ligands. Therefore, the local coordination environment around the Mn^{II} atom can be regarded as a slightly distorted octahedron with an N_2O_4 donor set. Each titmb ligand, in turn, connects three Mn atoms in cis, trans, trans-conformation (see Scheme 1).

Neglecting the interactions of Mn^{II} atoms with the oxalate anions and water molecules, Mn^{II} atoms are linked by titmb ligands to give an independent 1D stepwise chain, as shown in Figure S5 in the Supporting Information. A similar 1D stepwise chain has been observed in the previously reported complex, $[Cd_3(titmb)_2(SO_4)_4(H_2O)_2(CH_3CH_2OH)_2][Cd(H_2O)_6]{\cdot}2H_2O$, which was obtained via the reaction of the titmb ligand with $CdSO_4{\cdot}2.7H_2O$.[17b] The 1D chains were further linked by oxalate anions to generate a 2D network structure (Figure 4). The distances between Mn1 and Mn2, Mn2 and Mn3, and Mn3 and Mn4 are 5.57, 5.65, and 5.68 Å, respectively. The crystal packing diagram of **2** is illustrated in Figure S6 in the Supporting Information. The 2D layers were further linked by C−H···O and C−H···N hydrogen bonds to produce a 3D framework (see Figure S6 in the Supporting Information), and the noncoordinated water molecules are located in the voids formed between two adjacent cationic layers. The distances of 2.65−2.88 Å between the O atom of solvated water and the O atom of oxalate, or among the O atoms of the water molecules, indicate the presence of the O−H···O hydrogen bonds, although the H atoms of the water molecules could not be found in the difference Fourier map (see Table 3).

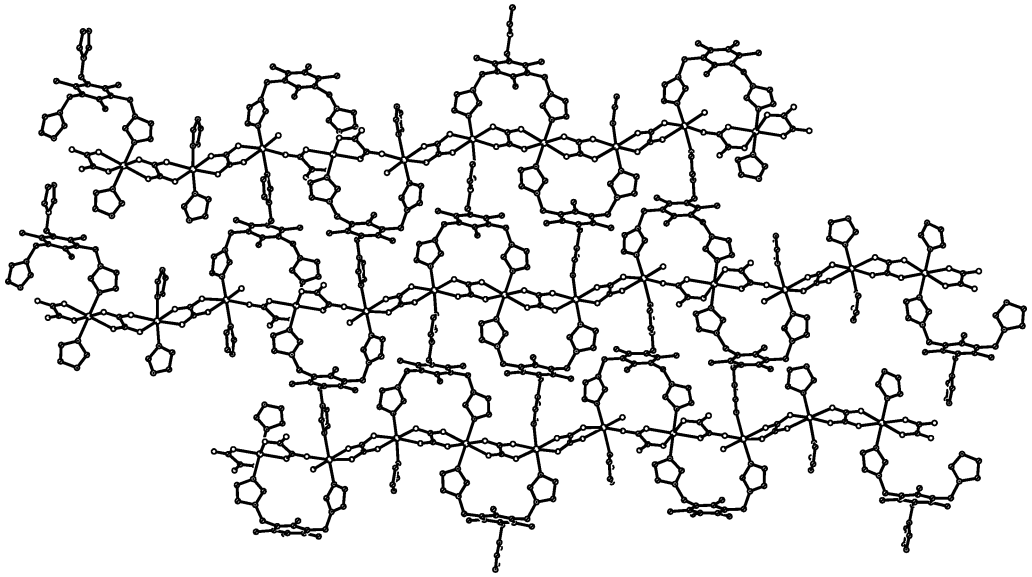

Figure 4. Two-dimensional (2D) network structure of complex **2** (the lattice water molecules and H atoms have been omitted for the sake of clarity).

In the previously reported complex, $[Mn(titmb)_2](SO_4)\cdot 16H_2O$ was obtained via the reaction of $MnSO_4\cdot H_2O$ with the ligand titmb, where each titmb was coordinated to three Mn^{II} atoms to give a 2D honeycomb network.[17b] The results showed that the anions with different coordination ability and bridging mode have remarkable impact on the structure of the MOFs.

3.2. Magnetic Properties of 1 and 2. Variable-temperature magnetic susceptibility measurements were performed on powder samples of **1** and **2** in the range of 300 K to 1.8 K. Figure 5a gives a plot of $\chi_M T$ versus temperature T for complex **1**. At room temperature, $\chi_M T$ is 3.89 emu K mol^{-1}, which is less than the spin-only value for the Mn(II) unit ($g = 2$ and $S = {}^5/_2$) (4.375 emu K mol^{-1}), suggesting the antiferromagnetic exchange between Mn^{II} ions. As the temperature is reduced, $\chi_M T$ smoothly decreases over the entire temperature region, indicating that the antiferromagnetic interaction between metal ions dominates the magnetic properties of **1**. In the plot of $\chi_M - T$ (Figure 5a), a maximum at 28 K was observed, which is the nature of the typical antiferromagnetic interaction between the magnetic centers. In the reduced-temperature region below 8 K, the increase of the magnetic susceptibility suggests the presence of the paramagnetic impurities in this complex. There are two types of bridging ligands—azide and titmb—in this complex. The former bridges the Mn^{II} ions by EE mode to form a 1D uniform chain, and then the titmb ligands connect the chains leading to the 3D structure of **1**. From a magnetic viewpoint, the EO azide bridging mode usually mediates ferromagnetic interaction[21,22] and the EE azide bridging mode mediates antiferromagnetic interaction.[21,23] The magneto-correlation of **1** also conformed to this universality, and the titmb ligands

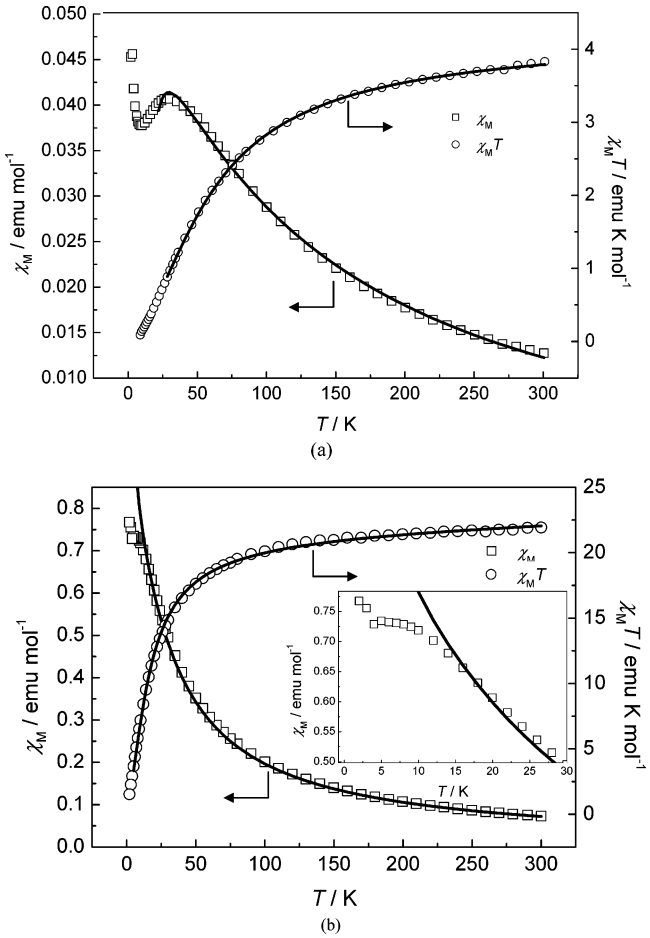

Figure 5. Plots of (○) the product $\chi_M T$ vs T and (□) χ_M vs T under an applied magnetic field of 2.0 kG for complexes (a) **1** and (b) **2**. Inset in panel b represents an enlarged view of the $\chi_M - T$ plot in the range of 30 K to 1.8 K for complex **2**.

are considered to have no contribution in mediating magnetically exchanged interactions between metal ions, because of the nonconjugated structure of titmb. To estimate the coupling interaction between the Mn^{II} ions, a 1D uniform chain model[24] with the Hamiltonian $\mathcal{H} = -J\Sigma \boldsymbol{S}_{2i}\boldsymbol{S}_{2i+1}$ was

(21) Comarmond, J.; Plumere, P.; Lehn, J.-M.; Agnus, Y.; Louis, R.; Weiss, R.; Kahn, O.; Morgenstern-Badarau, J. *J. Am. Chem. Soc.* **1982**, *104*, 6330.
(22) Boillot, M. L.; Journaux, Y.; Bencini, A.; Gatteschi, D.; Kahn, O. *Inorg. Chem.* **1985**, *24*, 263.
(23) Chaudhuri, P.; Oder, K.; Wieghardt, K.; Nuber, B.; Weiss, J. *Inorg. Chem.* **1986**, *25*, 2818.

used here. The best parameters in the range of 300 K to 20 K were obtained by a standard least-squares fitting program: $g = 2.05(2)$ and $J = -1.85(5)$ cm^{-1}, with $R = 1.2 \times 10^{-4}$ ($R = \sum[(\chi_M T)_{calc} - (\chi_M T)_{obs}]^2/\sum(\chi_M T)^2_{obs}$), which indicate the weak antiferromagnetic exchange between the Mn^{II} ions.

The plot of temperature dependence of magnetic properties of **2** is similar to that of **1** (see Figure 5b). At room temperature, $\chi_M T$ is 21.93 emu K mol^{-1}, which is consistent with the value of the five isolated Mn(II) ions with $g = 2$ and $S = {}^5/_2$ (21.875 emu K mol^{-1}). (The asymmetrical unit of the structure contains four Mn^{II} ions; however, a five Mn^{II}-ion unit is more advantageous for discussing the magnetic properties, as follows.) However, the maximum in the $\chi_M - T$ plot for **2** is 5 K, which is much lower than that for **1**. According to the magneto-structure, **2** may be considered as an alternating chain with $-(Mn_5-Mn)_n-$, as follows:

$$\text{- - - } Mn_1 \text{ - - - } zj' \text{ - - - } Mn_2 \overset{J_2}{-} Mn_3 \overset{J_1}{-} Mn_4 \overset{J_1}{-} Mn_{3A} \overset{J_2}{-} Mn_{2A} \text{ - - - } zj' \text{ - - - } Mn_{1A} \text{ - - -}$$

The crystal structure shows that the bridges between Mn2 and Mn3 and between Mn3 and Mn4 are not identical (see Figure 3). Therefore, the Hamiltonian for an approximate linear pentanuclear model is written as follows:

$$\mathscr{H} = -2J_2(\boldsymbol{S}_2\boldsymbol{S}_3 + \boldsymbol{S}_{3A}\boldsymbol{S}_{2A}) - 2J_1(\boldsymbol{S}_3\boldsymbol{S}_4 + \boldsymbol{S}_4\boldsymbol{S}_{3A})$$

i.e., $Mn_3-Mn_4-Mn_{3A}$ as a trimer cluster will produces eight spin states, $S_i = {}^1/_2, \ldots, {}^{15}/_2$.[25] The spin states then couple with the two terminal spins, $S = {}^5/_2$ at Mn_2 and Mn_{2A}. The final susceptibility can be written as eq 1:

$$\chi_m = \chi_m(S_i)P_{S_i}$$

and

$$P_{S_i} = \frac{(2S_i + 1)\exp\left(-\dfrac{E_i}{kT}\right)}{\sum(2S_i + 1)\exp\left(-\dfrac{E_i}{kT}\right)} \qquad (1)$$

where $\chi_m(S_i)$ is the molar susceptibility based on the spin state S_i coupling with Mn_2 and Mn_{2A} (see the Supporting Information) and P_{S_i} is the partition factor of the spin state S_i. Assuming the coupling interaction between Mn_1 and the pentanuclear is taken into account as zj' and $z = 2$, the mole magnetic susceptibility of **2** will be

$$\chi_M = \frac{\chi_m}{1 - (2zj'/Ng^2\beta^2)\chi_m} \qquad (2)$$

The best fitting by Matlab in the range of 300K to 5 K gives $g = 2.04$, $J_1 = -0.43$ cm^{-1}, $J_2 = -0.41$ cm^{-1}, and $zj' = -0.092$ cm^{-1} with $R = 6.40 \times 10^{-4}$. The results indicate the oxalate bridges and the carboxylate in syn−anti coordination mode mediate weak antiferromagnetic coupling[26] between Mn^{II} ions in **2**, which is comparable with those reported previously.[27]

Conclusions

Two novel complexes $[Mn(titmb)(N_3)_2]\cdot 1.5H_2O$ (**1**) and $[Mn_3(titmb)_2(C_2O_4)_3(H_2O)]\cdot 10H_2O$ (**2**) obtained by reactions of tripodal ligand 1,3,5-tris(imidazol-1-ylmethyl)-2,4,6-trimethylbenzene (titmb) with $Mn(OAc)_2\cdot 4H_2O$, together with NaN_3 and $K_2C_2O_4$, respectively, have been crystallographically and magnetically characterized. Because of the diversity of the azide and the oxalate ion in bridging metal ions, the metal-azide (oxalate) complexes with a specific co-ligand are expected to show various novel structures and interesting magnetic properties. In the present case, compounds **1** and **2**, obtained with the same co-ligand of titmb and under almost the same synthetic procedures, are distinct from each other, in regard to composition, topology, and magnetic properties. Complex **1** is a novel noninterpenetrating three-dimensional framework with an antiferromagnetic interaction between Mn^{II} ions in which the azide ligand bridges in an EE mode, and complex **2** has a two-dimensional network structure in which independent one-dimensional stepwise chains are linked by the oxalate ligand. Metal-organic frameworks (MOFs) with flexible or rigid tripodal ligands have been reported to have ionic/molecular recognition and ion exchange properties.[2,8,16] The present study reports, for the first time, the magnetic properties of MOFs with a flexible tripodal ligand. The structures and magnetic properties of **1** and **2** are a new demonstration of the remarkable versatility of the azide and oxalate ions in building new magnetic materials and illustrate the great challenges and opportunities in the fields of supramolecular chemistry and molecule-based magnetism.

Acknowledgment. This work was supported by the National Natural Science Foundation of China (Grant No. 20231020) and the National Science Fund for Distinguished Young Scholars (Grant No. 20425101). The authors are grateful to the anonymous referees for their kind suggestions on the interpretation of the magnetic properties.

Supporting Information Available: X-ray crystallographic file (CIF format). Schematic drawings and crystal packing diagrams for **1** and **2** (Figures S1−S6), and magnetic analysis for **2** (PDF format). This material is available free of charge via Internet at http://pubs.acs.org.

IC048816E

(24) Cortés, R.; Drillon, M.; Solans, X.; Lezama, L.; Rojo, T. *Inorg. Chem.* **1997**, *36*, 677.
(25) Kou, H.-Z.; Zhou, B. C.; Liao, D.-Z.; Wang, R.-J.; Li, Y. *Inorg. Chem.* **2002**, *41*, 6887.
(26) Kongshaug, K. O.; Fjellvåg, H. *Solid State Sci.* **2002**, *4*, 443.
(27) (a) Durot, S.; Policar, C.; Pelosi, G.; Bisceglie, F.; Mallah, T.; Mahy, J.-P. *Inorg. Chem.* **2003**, *42*, 8072 and references therein. (b) Policar, C.; Lambert, F.; Cesario, M.; Morgenstern-Badarau, I. *Eur. J. Inorg. Chem.* **1999**, 2201 and references therein.